

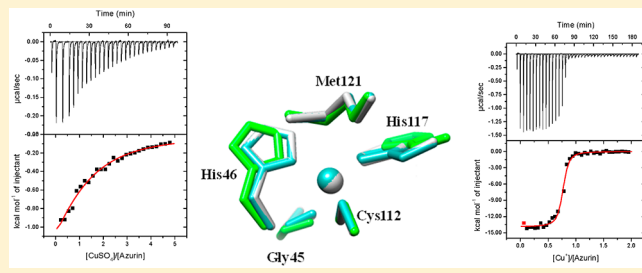
Shift from Entropic Cu²⁺ Binding to Enthalpic Cu⁺ Binding Determines the Reduction Thermodynamics of Blue Copper Proteins

Molly L. North[†] and Dean E. Wilcox*^{‡, ID}

Department of Chemistry, Dartmouth College, Hanover, New Hampshire 03755, United States

Supporting Information

ABSTRACT: The enthalpic and entropic components of Cu²⁺ and Cu⁺ binding to the blue copper protein azurin have been quantified with isothermal titration calorimetry (ITC) measurements and analysis, providing the first such experimental values for Cu⁺ binding to a protein. The high affinity of azurin for Cu²⁺ is entirely due to a very favorable binding entropy, while its even higher affinity for Cu⁺ is due to a favorable binding enthalpy and entropy. The binding thermodynamics provide insight into bond enthalpies at the blue copper site and entropic contributions from desolvation and proton displacement. These values were used in thermodynamic cycles to determine the enthalpic and entropic contributions to the free energy of reduction and thus the reduction potential. The reduction thermodynamics obtained with this method are in good agreement with previous results from temperature-dependent electrochemical measurements. The calorimetry method, however, provides new insight into contributions from the initial (oxidized) and final (reduced) states of the reduction. Since ITC measurements quantify the protons that are displaced upon metal binding, the proton transfer that is coupled with electron transfer is also determined with this method. Preliminary results for Cu²⁺ and Cu⁺ binding to the Phe114Pro variant of azurin demonstrate the insight about protein tuning of the reduction potential that is provided by the binding thermodynamics of each metal oxidation state.



INTRODUCTION

Metalloproteins and metalloenzymes typically bind their essential metal ion(s) with high affinity, thereby ensuring they maintain an active structure and/or catalytic activity. This is especially important for redox metalloproteins,¹ where both oxidation states of the metal must remain bound for their function in electron transfer. The protein affinity for a metal ion includes both enthalpic and entropic components that are unique for the protein site and the metal ion, and these originate from first coordination sphere bonding, second coordination sphere contributions (e.g., hydrogen bonding, electrostatic environment), and entropic factors (e.g., desolvation, conformational changes).

During electron transfer to a redox metalloprotein, the initial state has a bound oxidized metal ion, and the final state has a bound reduced metal ion. Since the two ions have a different charge and electronic structure, reduction involves a shift from the thermodynamics that bind the oxidized metal ion to the thermodynamics that bind the reduced metal ion. Therefore, the reduction thermodynamics of a metalloprotein can be determined from cycles that include the thermodynamics of binding each metal oxidation state to the protein. The reduction thermodynamics also includes contributions from the charge-balancing proton transfer that accompanies electron transfer.^{2–6}

A well-studied protein redox site is the blue copper, or type 1 copper, site found in small proteins (e.g., plastocyanin,⁷

azurin⁸) and multicopper oxidases (e.g., laccase,⁹ ascorbate oxidase¹⁰), which have trigonal copper coordination by a Cys thiolate and two His residues, as well as weak axial ligation, in both the oxidized (Cu²⁺) and reduced (Cu⁺) proteins, as shown for azurin (Figure 1).

This results in unique spectral ($\lambda_{\text{max}} \sim 600$ nm; $\varepsilon \sim 5000$ M⁻¹ cm⁻¹) and magnetic (small A_{\parallel} hyperfine coupling) properties of Cu²⁺ bound at this protein site, which has a higher reduction potential (~ 180 –370 mV vs NHE) than aqueous copper (150 mV vs NHE). Rapid electron transfer by this metalloprotein site is due, in large part, to the small inner-sphere reorganization for the similar Cu²⁺ and Cu⁺ coordinations.^{11,12} Of particular relevance here, a very similar structure of the active site residues is maintained in the metal-free apo-protein,^{13–15} resulting in little conformational change upon either Cu²⁺ or Cu⁺ binding (Figure 1).

We have used isothermal titration calorimetry (ITC) measurements to quantify the thermodynamics of both Cu²⁺ and Cu⁺ binding to azurin. These results are compared with Cu²⁺ binding thermodynamics reported earlier¹⁶ and provide the first thermodynamics of Cu⁺ binding to a protein. We find that each metal ion binds to azurin with a unique and very different combination of enthalpy and entropy, which provides insight about Cu²⁺ and Cu⁺ bonding at the blue copper site

Received: June 27, 2019

Published: August 21, 2019

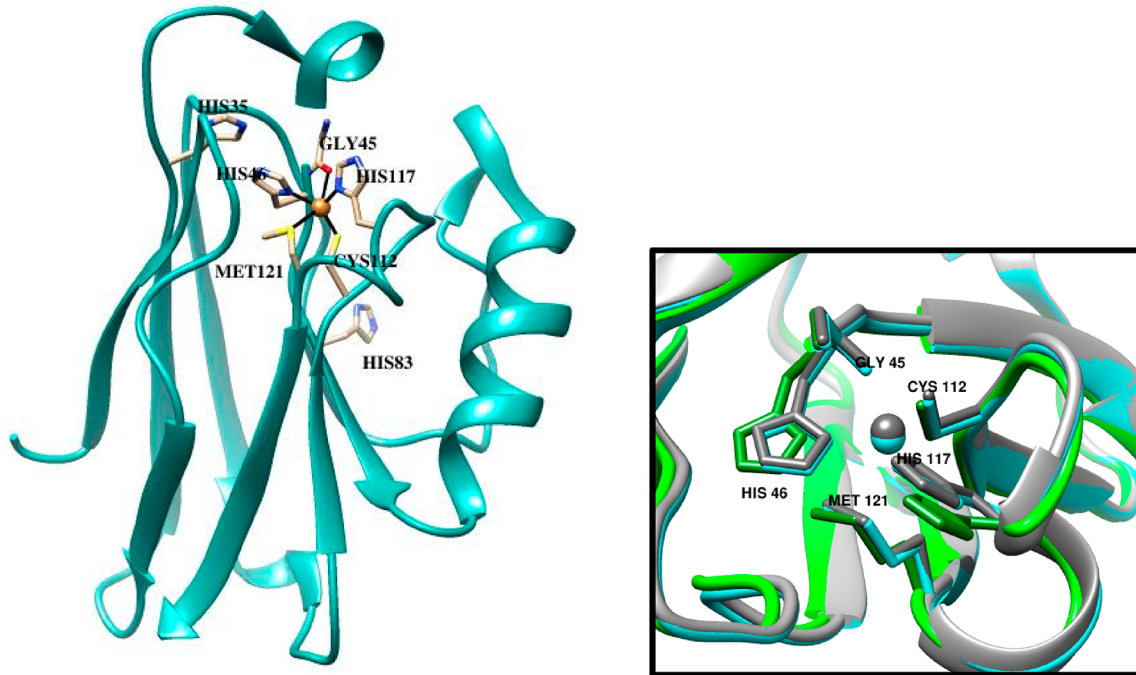


Figure 1. Structures of *P. aeruginosa* azurin (left) wild-type Cu²⁺-azurin (PDB 4AZU), with metal-coordinating and other key residues indicated; (right) overlay of the metal-binding site for Cu²⁺-azurin (blue; PDB 4AZU), Cu⁺-azurin (gray; PDB 1E5Y), and apo-azurin (green; PDB 1E65).

and entropic contributions to the protein affinity for each metal ion. The binding thermodynamics were then used in thermodynamic cycles to determine the azurin reduction thermodynamics for comparison to values reported previously from temperature-dependent electrochemical measurements of the reduction potential.^{17,18} Since ITC measurements quantify the proton transfer to/from the protein that accompanies metal binding, these results for Cu²⁺ and Cu⁺ were used to experimentally quantify the proton transfer that is coupled to the electron transfer of azurin reduction. Finally, preliminary measurements and analysis of an azurin variant provide an example of the quantitative insight about protein tuning of the metal reduction potential that can be determined with this calorimetric method.

EXPERIMENTAL SECTION

Pseudomonas aeruginosa azurin DNA was provided in a pET9a vector from Yi Lu (University of Illinois Urbana—Champaign), with permission from the late John Richards (California Institute of Technology), as was the DNA of the F114P mutant.

The expression and purification procedure for both wild-type and F114P azurin was adapted from Karlsson et al.¹⁹ (see *Supporting Information*).

Copper was removed from azurin by dialysis of the holo-protein against 0.15 M Tris, 0.10 M KCN, and pH 8.3, at 4 °C overnight (~8 h minimum).^{20,21} The resulting apo-azurin was then exchanged into the buffer of interest by centrifugal filtration with a 10K Amicon filter (EMD Millipore) until no more cyanide was detected. The protein concentration was determined by A_{280} with $\epsilon = 9 \text{ mM}^{-1} \text{ cm}^{-1}$.²²

Stock solutions of Cu⁺ were prepared by comproportionation from CuSO₄ and copper wire, as described previously,²³ with excess 1,1,4,7,10,10-hexamethyltriethylenetetramine (Me₆Trien) (Sigma-Aldrich) as the Cu⁺-stabilizing ligand and the final pH adjusted to neutral. All solutions were prepared with deoxygenated distilled (18 MΩ) water in an anaerobic Coy chamber with a 98% N₂ and 1.5% H₂ atmosphere and a Pd catalyst that kept the oxygen level at ≤2 ppm. The concentration of Cu⁺ was determined spectrophotometrically with a bicinchoninic acid (BCA) standard and A_{563} , with $\epsilon = 7.9$

$\text{mM}^{-1} \text{ cm}^{-1}$ for the resulting Cu(BCA)₃.²⁴ Buffer solutions were evacuated and sparged with Ar prior to use.

The ITC samples were prepared immediately prior to measurement in glass vials that had been acid washed to remove trace metals. Anaerobic samples of apo-azurin for Cu⁺ titrations were prepared in one of two ways: (a) dithiothreitol was added to a 2.5 mL concentrated sample of apo-azurin to a final concentration of ~3 mM in the anaerobic Coy chamber, and this solution was added to a PD-10 desalting column (GE Healthcare) that had been equilibrated with the degassed buffer of interest, and the protein was eluted with 3 mL of the same buffer or (b) a concentrated solution of apo-azurin was evacuated until bubbles stopped appearing and was then taken into the anaerobic Coy chamber. Samples prepared with either method gave quantitatively similar ITC results.

The ITC measurements were obtained with a MicroCal VP-ITC that has a 1.4 mL sample cell and 300 μL injection syringe, using 7–10 μL injection volumes, 300–600 s injection spacings, 459 rpm stirring, and 25 °C. Both the titrant (metal ion) and titrand (protein) were in identical buffered solutions. For anaerobic measurements, the VP-ITC was housed in a custom Plexiglas glovebox that was purged with N₂ gas. The ITC measurements are presented in a top panel that shows the raw data (power vs time), with negative exothermic peaks and positive endothermic peaks and a bottom panel that shows the integrated, concentration-normalized enthalpy plotted against the molar ratio of titrant (syringe) to titrand (cell). The data were fit to a one-site binding model provided with the VP-ITC Origin software.

Initial measurements for each type of experiment were used to determine the conditions (sample concentrations; injection volume, spacing, number) necessary to provide thermograms that were consistent and suitable for analysis. A minimum of three measurements was then obtained and analyzed, with errors calculated from standard deviations of the data from these titrations.

A *post hoc* analysis of the experimental binding enthalpy (ΔH_{ITC}) accounted for the contributions from buffer competition for Cu²⁺ and Me₆Trien competition for Cu⁺, as well as protonation of the buffer and Me₆Trien. This required the thermodynamics of buffer interaction with Cu²⁺ ($\Delta H^{\circ}_{\text{Cu2+}-\text{buffer}}$), described in Appendix A of the *Supporting Information*, and the thermodynamics of formation of the Cu⁺ complex with Me₆Trien ($\Delta H^{\circ}_{\text{Cu+}-\text{Me6Trien}}$), described in Appendix B of the *Supporting Information*. This analysis also

quantifies the protonation of the buffer, which is needed to determine $\Delta H^\circ_{\text{Cu-Azurin}}$ using a Hess's Law analysis for Cu^{2+} (eq 1) and Cu^+ (eq 2).

$$\begin{aligned} \Delta H_{\text{ITC}} = & -\Delta H^\circ_{\text{Cu}^{2+}-\text{buffer}} - n_{\text{H}^+}\Delta H^\circ_{\text{Azurin-H}} + n_{\text{H}^+}\Delta H^\circ_{\text{buffer-H}} \\ & + \Delta H^\circ_{\text{Cu}^{2+}-\text{Azurin}} \end{aligned} \quad (1\text{a})$$

$$\begin{aligned} \Delta H_{\text{ITC}} + \Delta H^\circ_{\text{Cu}^{2+}-\text{buffer}} = & n_{\text{H}^+}(\Delta H^\circ_{\text{buffer-H}}) \\ & + (-n_{\text{H}^+}\Delta H^\circ_{\text{Azurin-H}} + \Delta H^\circ_{\text{Cu}^{2+}-\text{Azurin}}) \end{aligned} \quad (1\text{b})$$

$$\begin{aligned} \Delta H_{\text{ITC}} = & -\Delta H^\circ_{\text{Cu}^+-\text{Me}_6\text{Trien}} - n_{1\text{H}^+}\Delta H^\circ_{\text{Azurin-H}} \\ & + n_{2\text{H}^+}\Delta H^\circ_{\text{Me}_6\text{Trien-H}} + n_{3\text{H}^+}\Delta H^\circ_{\text{buffer-H}} \\ & + \Delta H^\circ_{\text{Cu}^+-\text{Azurin}} \end{aligned} \quad (2\text{a})$$

$$\begin{aligned} \Delta H_{\text{ITC}} + \Delta H^\circ_{\text{Cu}^+-\text{Me}_6\text{Trien}} = & n_{3\text{H}^+}(\Delta H^\circ_{\text{buffer-H}}) + n_{2\text{H}^+}\Delta H^\circ_{\text{Me}_6\text{Trien-H}} \\ & + (-n_{1\text{H}^+}\Delta H^\circ_{\text{Azurin-H}} + \Delta H^\circ_{\text{Cu}^+-\text{Azurin}}) \end{aligned} \quad (2\text{b})$$

In the case of Cu^{2+} (eq 1a), protons displaced from the protein (n_{H^+}) bind to the buffer. For Cu^+ (eq 2a), the displaced protons ($n_{1\text{H}^+}$) bind first to the Me_6Trien that has released the Cu^+ ($n_{2\text{H}^+}$) since it has higher $\text{p}K_a$ values (9.19, 8.38) than the buffer, and additional displaced protons bind to the buffer ($n_{3\text{H}^+}$) (Appendix B). Buffer protonation upon Cu^{2+} (n_{H^+}) and Cu^+ ($n_{3\text{H}^+}$) binding to azurin was quantified by an analysis of the binding data in different buffers using the linear relationships in eq 1b and eq 2b, respectively.

A *post hoc* analysis of the experimental binding constant (K_{ITC}) accounts for buffer competition for Cu^{2+} (eq 3) and competition by Me_6Trien for Cu^+ , where proton competition with Cu^+ for Me_6Trien is also included in the analysis (eq 4).^{23,25} This provides the condition-independent binding constant ($K_{\text{Cu-Azurin}}$).

$$K_{\text{Cu}^{2+}-\text{Azurin}} = K_{\text{ITC}}(\alpha_{\text{buffer}}) = K_{\text{ITC}}(1 + K_{\text{Cu}^{2+}-\text{buffer}}[\text{buffer}]_{\text{basic}}) \quad (3)$$

$$\begin{aligned} K_{\text{Cu}^+-\text{Azurin}} = & K_{\text{ITC}}(\alpha_{\text{Me}_6\text{Trien}}) \\ = & K_{\text{ITC}}\left(1 + K_{\text{Cu}^+-\text{Me}_6\text{Trien}} \frac{[\text{Me}_6\text{Trien}]_{\text{total}}}{(1 + K_{\text{Me}_6\text{Trien-H}}[\text{H}^+])}\right) \end{aligned} \quad (4)$$

The change in free energy (ΔG°) and entropy (ΔS°) for metal ion binding to the protein is then found with standard relationships (eq 5).

$$\begin{aligned} \Delta G^\circ_{\text{Cu-Azurin}} = & -RT \ln K_{\text{Cu-Azurin}} \\ = & \Delta H^\circ_{\text{Cu-Azurin}} - T\Delta S^\circ_{\text{Cu-Azurin}} \end{aligned} \quad (5)$$

Thermodynamic values are referenced to the biochemical standard state (pH 7.0), ΔX° , as is common for biomolecular calorimetry.

RESULTS AND ANALYSIS

Cu²⁺ Binding to Azurin. Copper(II) binding to apo-azurin was measured by ITC at pH 7.0 and 25 °C in four different buffers. Figure 2 shows representative data for a $\text{Cu}^{2+} \rightarrow$ apo-azurin titration with both the metal ion and protein in a 100 mM bis-Tris buffer solution.

Similar binding isotherms are found for reverse titrations (apo-azurin \rightarrow Cu^{2+}) in matched buffer solutions. The metal-binding stoichiometry was very close to the expected value of 1.0 with some buffers, but this value was fixed for others. The binding appears to be weak for a metalloprotein, but the isotherm reflects the competition between the protein and the amine buffer, which has a significant affinity for Cu^{2+} .

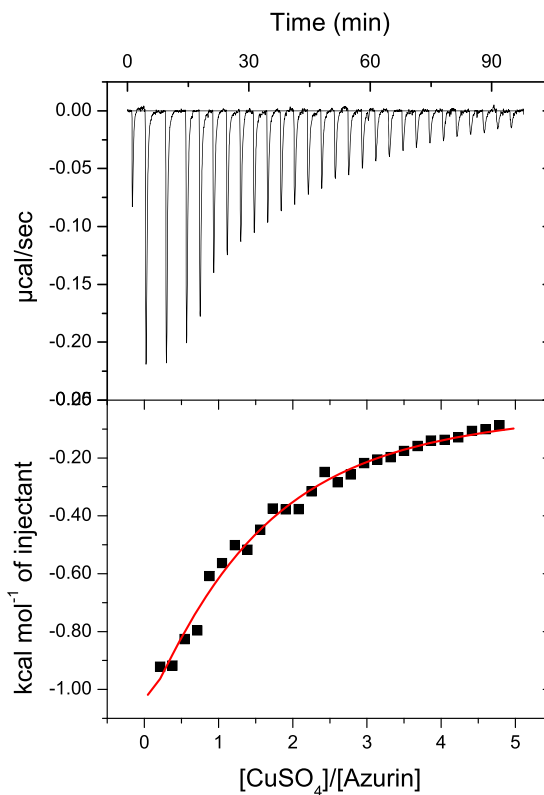


Figure 2. Representative ITC thermogram of 1.0 mM CuSO_4 titrated into 0.03 mM apo-azurin with both solutions containing 100 mM bis-Tris buffer, 100 mM NaCl, pH 7.0; best fit values to a one-site binding model: $n = 1.0 \pm 0.2$, $K_{\text{ITC}} = 2.5 (\pm 0.4) \times 10^4$, $\Delta H_{\text{ITC}} = -2.4 \pm 0.5 \text{ kcal mol}^{-1}$.

(Appendix A) and is present at a high concentration. Table 1 contains the average values from best fits of the experimental data to a one-site binding model.

Further analysis of the binding data requires the quantification of proton transfer to/from the buffer that is coupled with Cu^{2+} binding to the protein. The experimental binding enthalpy in the four buffers, along with values for the enthalpy of the Cu^{2+} -buffer interaction (Appendix A) and the buffer protonation enthalpies,²⁶ were used in this analysis (Figure S1), which shows that 1.5 ± 0.3 protons are displaced from azurin upon Cu^{2+} binding at pH 7.0. This value was then used in a Hess's Law analysis of the data obtained with each buffer to determine the buffer-independent enthalpy of Cu^{2+} binding to azurin (Table 2). These values from data obtained with each buffer are quite similar, indicating that buffer contributions to the net binding enthalpy have been removed.

To determine the buffer-independent binding constant and binding free energy, competition by the basic form of the buffer for the Cu^{2+} at pH 7.0 (Appendix A) was included in the data analysis (eq 3). Again, the buffer-independent binding constants from data obtained with each buffer are quite similar (Table 2), indicating that buffer contributions to the free energy of metal binding have also been removed. These results reveal that Cu^{2+} binds to azurin with $\log K = 15.4 \pm 0.2$ ($K_D = 0.4 \pm 0.2 \text{ fM}$) and thermodynamic values of $\Delta G^\circ = -21.1 \pm 0.2 \text{ kcal/mol}$, $\Delta H^\circ = 2 \pm 1 \text{ kcal/mol}$, and $\Delta S^\circ = 78 \pm 3 \text{ cal/mol}\text{K}$ ($-T\Delta S^\circ = -23 \pm 1 \text{ kcal/mol at 298 K}$) at pH 7.0.

Cu⁺ Binding to Azurin. Copper(I) binding measurements in aqueous solution are more challenging due to competing oxidation, precipitation, and disproportionation reactions of

Table 1. Average Experimental ITC Values Obtained from Best Fits to a One-Site Binding Model for Cu^{2+} and Cu^+ Binding to Apo-Azurin in Different Buffers at pH 7.0 and 25 °C

	buffer	<i>n</i>	K_{ITC}	ΔH_{ITC} (kcal/mol)
Cu^{2+}	bis-Tris	1.03 ± 0.04	$2.1 (\pm 0.3) \times 10^4$	-2.4 ± 0.2
	TAPSO	1.04 ± 0.08	$7.8 (\pm 5.2) \times 10^4$	-2.04 ± 0.02
	DIPSO	1.00	$2.2 (\pm 1.1) \times 10^4$	-1.9 ± 0.3
	TES	1.00	$1.0 (\pm 0.5) \times 10^4$	-5.3 ± 0.7
Cu^+	HEPES	0.8 ± 0.1	$1.4 (\pm 0.7) \times 10^7$	-13.8 ± 0.8
	PIPES	0.8 ± 0.1	$1.3 (\pm 1.4) \times 10^8$	-12.6 ± 1.2
	ACES	0.56 ± 0.02	$8.0 (\pm 3.0) \times 10^7$	-13.7 ± 0.3
	TES	0.49 ± 0.01	$2.91 (\pm 0.03) \times 10^7$	-14.2 ± 0.6
	TAPSO	0.5 ± 0.1	$2.3 (\pm 1.8) \times 10^7$	-15.5 ± 0.9

Table 2. Buffer-Independent Thermodynamic Values for Cu^{2+} and Cu^+ Binding to Apo-Azurin at pH 7.0 and 25 °C

	buffer	<i>n</i>	$\log K_{\text{MP}}$	ΔG° (kcal/mol)	ΔH_{MP} (kcal/mol)	$-T\Delta S$ (kcal/mol)	ΔS (cal/(mol K))
Cu^{2+}	bis-Tris	1.03 ± 0.04	15.2 ± 0.3	-20.8 ± 0.4	0.8 ± 0.4	-21.6 ± 0.6	72 ± 2
	TAPSO	1.04 ± 0.08	15.9 ± 0.4	-21.7 ± 0.5	2.8 ± 2.0	-24.5 ± 2.1	82 ± 7
	DIPSO	1.00	14.9 ± 0.4	-20.4 ± 0.5	2.8 ± 0.5	-23.2 ± 0.7	78 ± 3
	TES	1.00	15.6 ± 0.4	-21.3 ± 0.5	2.0 ± 1.0	-23.3 ± 1.1	78 ± 4
	average		15.4 ± 0.2	-21.1 ± 0.2	2 ± 1	-23 ± 1	78 ± 3
Cu^+	HEPES	0.8 ± 0.1	17.1 ± 0.5	-23.4 ± 0.7	-17.6 ± 1.0	-5.8 ± 1.2	20 ± 4
	PIPES	0.8 ± 0.1	18.1 ± 0.6	-24.7 ± 0.9	-17.2 ± 1.3	-7.5 ± 1.6	25 ± 5
	ACES	0.56 ± 0.02	17.9 ± 0.4	-24.5 ± 0.6	-16.3 ± 0.7	-8.2 ± 0.9	27 ± 3
	TES	0.49 ± 0.01	17.5 ± 0.4	-23.9 ± 0.6	-17.3 ± 0.8	-6.6 ± 1.0	22 ± 3
	TAPSO	0.5 ± 0.1	17.4 ± 0.5	-23.7 ± 0.7	-18.1 ± 1.1	-5.6 ± 1.3	19 ± 5
	average		17.6 ± 0.2	-24.0 ± 0.3	-17 ± 1	-7 ± 1	23 ± 2

this metal ion, all of which must be suppressed. This can be achieved by anaerobically delivering the Cu^+ from a well-characterized complex with a ligand that stabilizes this metal ion, and Me_6Trien (1,1,4,7,10,10-hexamethyltriethylenetetramine) served this role here.²⁷ Copper(1) binding to apo-azurin was measured by ITC in five different buffers containing a ~50-fold excess of Me_6Trien at pH 7.0 and 25 °C, with Figure 3 showing representative data for a $\text{Cu}^+ \rightarrow$ apo-azurin titration with both titrant and titrand in a 100 mM HEPES buffer solution.

The binding isotherm reflects the difference between the affinity of the protein for Cu^+ and the stability of the Cu^+ – Me_6Trien complex. Average values from best fits of the experimental data to a one-site binding model are found in Table 1.

The binding stoichiometry with some buffers is close to the expected value of 1.0, but the value is lower and closer to 0.5 for other buffers. Values less than 1.0 indicate protein oxidation, or degradation, but the lower stoichiometry with certain buffers suggests a unique interaction with the Cu^+ – Me_6Trien complex and/or the protein. While data in two piperazine-based buffers (HEPES, PIPES) give values close to 1.0, data in three secondary amine buffers (ACES, TES, TAPSO) have lower stoichiometries. However, ITC data are normalized to the amount of titrant added, and all five buffers give very similar condition-independent thermodynamic values for Cu^+ binding to azurin.

Further analysis of the binding data again requires the quantification of proton transfer to/from the buffer that is coupled with Cu^+ binding to the protein. The experimental binding enthalpies in the five buffers, along with values for the buffer protonation enthalpies,²⁶ were used in this analysis (Figure S2), which shows that 0.3 ± 0.1 protons are displaced to the buffer upon Cu^+ binding to azurin at pH 7.0. This value

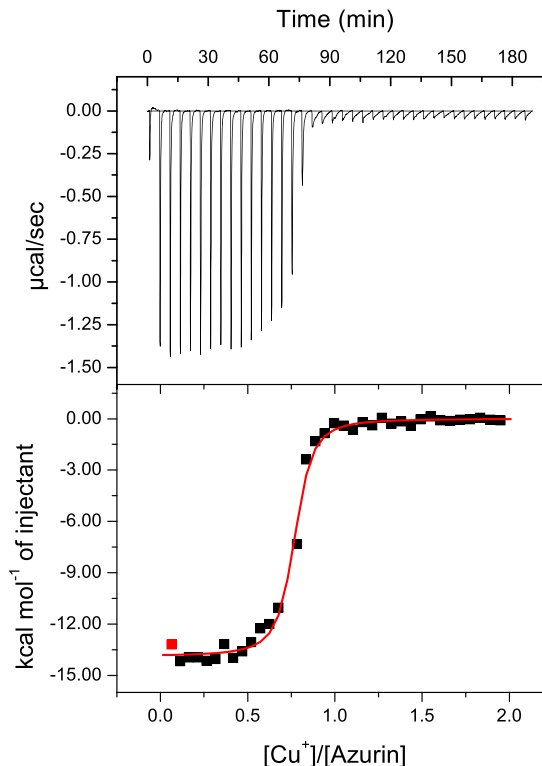


Figure 3. Representative ITC thermogram of 0.3 mM Cu^+ /16.5 mM Me_6Trien titrated into 0.03 mM apo-azurin/16.5 mM Me_6Trien with both solutions containing 100 mM HEPES buffer, 100 mM NaCl, and pH 7.0; best fit values to a one-site binding model: $n = 0.75 \pm 0.01$, $K_{\text{ITC}} = 9.8 (\pm 1.7) \times 10^6$, $\Delta H_{\text{ITC}} = -13.9 \pm 0.1$ kcal mol⁻¹.

was then used in a Hess's Law analysis of the data in each buffer to determine the buffer-independent enthalpy of Cu^+

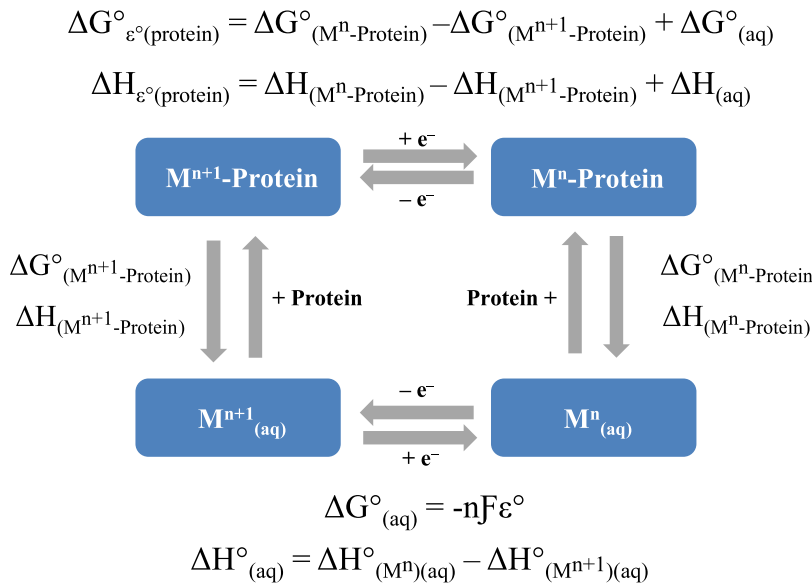


Figure 4. Thermodynamic cycles to determine the reduction free energy and reduction enthalpy of a metalloprotein with calorimetric measurements of the oxidized and reduced metal ion binding to the protein.

binding to azurin (Table 2). The analysis includes the protonation of Me_6Trien upon its release from the Cu^+ and required a careful evaluation of the protonation state, stability, and formation enthalpy of the Me_6Trien complex with Cu^+ at pH 7.0 (Appendix B). The metal-binding enthalpies obtained from data with each buffer are quite similar, indicating that buffer contributions to the net binding enthalpy have been removed.

To determine the Cu^+ binding constant and binding free energy, the competition by Me_6Trien for the Cu^+ at pH 7.0 was included in the data analysis (eq 4). Since Me_6Trien has two higher pK_a 's (9.19, 8.38), this involves proton competition with Cu^+ for this ligand, which is included in the analysis. The condition-independent binding constants obtained from data with each of the buffers are similar (Table 2), indicating a consistent analysis of the experimental data under different conditions. These results reveal that Cu^+ binds to azurin with $\log K = 17.6 \pm 0.2$ ($K_D = 2 \pm 1 \text{ aM}$) and thermodynamic values of $\Delta G^{\circ} = -24.0 \pm 0.3 \text{ kcal/mol}$, $\Delta H^{\circ} = -17 \pm 1 \text{ kcal/mol}$, and $\Delta S^{\circ} = 23 \pm 2 \text{ cal/mol}\cdot\text{K}$ ($-T\Delta S^{\circ} = -7 \pm 1 \text{ kcal/mol}$ at 298 K) at pH 7.0.

Thermodynamics of Azurin Reduction. With thermodynamic values for Cu^{2+} and Cu^+ binding to apo-azurin, it is now possible to determine the change in free energy ($\Delta G^{\circ}_{E^{\circ}}$) and the change in enthalpy ($\Delta H^{\circ}_{E^{\circ}}$) for azurin reduction from thermodynamic cycles (Figure 4).

Using the above values from the analysis of ITC data and the thermodynamic values for the reduction of $\text{Cu}^{2+}_{\text{aq}}$ to Cu^+_{aq} ($\Delta G^{\circ}_{E^{\circ}} = -3.5 \text{ kcal/mol}$, from $E^{\circ} = 150 \text{ mV}$ vs NHE, and $\Delta H^{\circ}_{E^{\circ}} = -3.0 \pm 0.1 \text{ kcal/mol}$, from the difference between the formation enthalpies of $\text{Cu}^{2+}_{\text{aq}}$ and Cu^+_{aq}),²⁸ we calculate $\Delta G^{\circ}_{E^{\circ}} = -6.4 \pm 0.4 \text{ kcal/mol}$ and $\Delta H^{\circ}_{E^{\circ}} = -22 \pm 1 \text{ kcal/mol}$. This reduction free energy corresponds to a reduction potential of $279 \pm 16 \text{ mV}$ vs NHE. While this value is somewhat lower than other reported azurin reduction potentials, it is consistent with the value reported for azurin samples obtained from the expression vector used in this study, $265 \pm 19 \text{ mV}$ vs NHE.²⁹ The change in entropy for the reduction of azurin can be determined from the change in free energy and enthalpy for azurin reduction ($\Delta S^{\circ}_{E^{\circ}} = -52 \pm 5 \text{ J/K}$).

kcal/mol·K) or from a thermodynamic cycle for the change in entropy ($\Delta S^{\circ}_{E^{\circ}} = -53 \text{ kcal/mol}\cdot\text{K}$).

Cu^{2+} and Cu^+ Binding to the F114P Variant and Its Reduction Thermodynamics. Following the procedures and analysis outlined above for wild-type azurin, ITC measurements were obtained for Cu^{2+} and Cu^+ (stabilized by Me_6Trien) binding to the apo F114P azurin variant in two different buffers at pH 7.0 (Figure S3). These data provide average experimental values (Table S1) that were used to determine the Cu^{2+} and Cu^+ binding thermodynamics (Table S2) for comparison to the binding thermodynamics of the wild-type protein (Table 3).

Table 3. Difference in the Metal Binding Thermodynamics between Wild-Type and F114P Azurin at pH 7.0 and 25 °C

	ΔG° (kcal/mol)	$\Delta \Delta H^{\circ}$ (kcal/mol)	$\Delta \Delta S^{\circ}$ (cal/(mol K))	$-T\Delta \Delta S^{\circ}$ (kcal/mol)
Cu^{2+}	-0.3 ± 0.4	-11 ± 1	-38 ± 5	11.3 ± 1.5
Cu^+	2.4 ± 0.5	4 ± 1	5 ± 5	-1.5 ± 1.5

As above, these values were used in thermodynamic cycles to determine the reduction thermodynamics of this variant, which has a reduction potential ($E^{\circ} = 171 \pm 7 \text{ mV}$ vs NHE)²⁹ that is $\sim 100 \text{ mV}$ lower than that of the wild-type protein. Table 4 compares the reduction thermodynamics of wild-type and F114P azurin.

■ DISCUSSION

The essential metal ion(s) of metalloproteins and metalloenzymes are typically bound with high affinity, which is particularly important for redox metalloproteins, such as those with the blue copper or type 1 copper site, where both oxidation states of the metal need to be bound tightly. We have used ITC measurements of the well-studied protein azurin from *Pseudomonas aeruginosa* and a detailed analysis of the calorimetry data to (a) obtain new insight into Cu^{2+} and Cu^+ bonding at the blue copper site, (b) reveal how the reduction potential is determined by the thermodynamics of each metal oxidation state bound to the protein, and (c) quantify the

Table 4. Thermodynamic Values for the Reduction of Wild-Type and F114P Azurin at pH 7.0 and 25 °C Obtained with ITC Data and Thermodynamic Cycles

azurin	$\Delta H^{\circ'}_{E^{\circ'}}$ (kcal/mol)	$\Delta S^{\circ'}_{E^{\circ'}}$ (cal/(mol K))	$\Delta G^{\circ'}_{E^{\circ'}}$ (kcal/mol)	$E^{\circ'}$ (mV)	E° from electrochemical methods (mV)
WT	-22 ± 1	-52 ± 5	-6.4 ± 0.4	279 ± 16	$\sim 310^{a,b}$ 265 ± 19^{c}
F114P	-7 ± 1	-11 ± 5	-3.7 ± 0.5	162 ± 22	171 ± 7^{c}

^aRef 17. ^bRef 47. ^cRef 29.

proton transfer that is coupled to the electron transfer of reduction.

Thermodynamics of Copper Binding to Azurin.

1. Earlier Results. Azurin and other blue copper proteins are known to bind Cu^{2+} tightly, requiring ligands with high copper affinity for removal. An earlier study used ITC measurements to estimate the binding thermodynamics and found a biphasic heat flow with each injection, indicating a two-step binding mechanism.¹⁶ The buffer for these measurements was cholamine chloride ($[\text{H}_2\text{NCH}_2\text{CH}_2\text{N}(\text{CH}_3)_3]\text{Cl}$), which was expected to have minimal interaction with the Cu^{2+} ions due to its positively charged quaternary amine. Further, the measurements involved titrating apo–azurin into a dilute Cu^{2+} solution to ensure solubility of the metal ion. We are able to reproduce the published data, including the biphasic injections, by carefully following the reported experimental conditions (Figure S4). In addition, we have investigated cholamine buffer and found that it has a significant and complex interaction with Cu^{2+} , possibly involving hydroxo species.³⁰ Since the earlier ITC data could only provide a lower limit for the binding constant, the free energy of Cu^{2+} binding to azurin was estimated from contributions to the binding entropy (desolvation, conformation, cratic) and the experimental binding enthalpy, which gave a reported azurin affinity for Cu^{2+} of $\log K = 13.6$ ($K_D = 25$ fM) and Cu^{2+} binding thermodynamics of $\Delta G^{\circ'} = -18.8$ kcal/mol, $\Delta H^{\circ'} = -10.2 \pm 1.6$ kcal/mol, and $\Delta S^{\circ'} = 29$ cal/mol·K ($-T\Delta S^{\circ'} = -8.6$ kcal/mol at 298 K).¹⁶

A subsequent study used spectrophotometric measurements of the competition between cyclam (1,4,8,11-tetraazacyclotetradecane) and azurin for Cu^{2+} and reported an exceptionally high Cu^{2+} affinity of $\log K = 24$ ($\Delta G^{\circ'} = -32.8 \pm 1.9$ kcal/mol),³¹ which was compared to a calculated binding free energy of $\Delta G^{\circ'} = -32.7 \pm 0.7$ kcal/mol.³² These values are not consistent with other reported values, including the one determined here.

The affinity of azurin for Cu^+ has been reported to be $\log K = 16.5$ ($K_D = 30$ aM), based on its reported affinity for Cu^{2+} from the earlier ITC measurements ($\log K = 13.6$)¹⁶ and a thermodynamic cycle that included the reduction potentials of azurin (320 mV vs NHE) and the aqueous cupric ion (150 mV vs NHE).³³ Based on these two potentials, the affinity of azurin for Cu^+ must be about 3 orders of magnitude higher than its affinity for Cu^{2+} , as we have found with ITC measurements of each metal ion binding to the protein.

A recent study used equilibrium competition and spectrophotometric measurements to determine the Cu^+ affinities of several copper trafficking and Cu-requiring proteins from the cyanobacterium *Synechocystis* and reported the affinity of its blue copper protein plastocyanin (Pc) for both Cu^+ and Cu^{2+} at pH 7.0.³⁴ The value for Cu^{2+} ($\log K = 14.7$) was determined by competition with the amino acid His, which forms the $\text{Cu}^{\text{II}}(\text{His})_2$ complex, and the value for Cu^+ ($\log K = 17.4$) was determined by competition with bathocuproine

disulfonate (BCS), which forms the $\text{Cu}^{\text{I}}(\text{BCS})_2^{-3}$ complex. These affinities are very similar to those determined here for azurin from ITC measurements. It was reported, however, that several hours were required to reach equilibrium for both Cu^{2+} and Cu^+ binding to Pc. We, and the previous ITC study,¹⁶ find that azurin binds these metal ions fast enough for the enthalpy measurements to reach equilibrium after each injection. Rapid stirring in the titration calorimeter clearly accelerates the binding. Further, Cu^+ exchange between the less stable 1:1 Me_6Trien complex ($\log K = 13.6 \pm 0.4$) and azurin may be faster than Cu^+ equilibration between the more stable 1:2 BCS complex ($\log \beta_2 = 19.4$) and Pc. For Cu^{2+} , Pc competition with the chelating His amino acid is expected to be slower than azurin competition with the monodentate amine buffers. Finally, different axial bonding in the Pc and azurin sites may contribute to different kinetics of metal binding.

2. Our Results. Our approach to quantifying the thermodynamics of Cu^{2+} and Cu^+ binding to azurin include ITC measurements of metal ion titrations into apo–azurin in several buffers. This is followed with a *post hoc* analysis that subtracts the known interaction of the metal ion with the buffer or Cu^+ -stabilizing ligand, which competes with the protein, and accounts for the contributions of proton displacement upon metal binding.²⁵

The number of protons that is displaced from a protein upon metal binding can be determined from an analysis of ITC data collected in multiple buffers and is found here to be 1.5 ± 0.3 for Cu^{2+} and 0.6 ± 0.1 for Cu^+ (0.3 ± 0.1 to the buffer and 0.28 ± 0.04 to the Me_6Trien that releases the Cu^+) binding to azurin at pH 7.0. Since $\text{p}K_a$ values have been determined for the three metal-binding residues (>8.2 for Cys112; 7.6 ± 0.1 for His117; <5.0 for His46) in apo–azurin and for two other key residues, His35 and His83, in the oxidized (Cu^{2+}), reduced (Cu^+), and apo protein,^{20,35} their protonation states are known at pH 7.0 (Table S3). This allows a proton inventory to predict that 1.74 ± 0.15 and 1.21 ± 0.15 protons should be displaced when Cu^{2+} and Cu^+ bind to azurin, respectively. The predicted number for Cu^{2+} is within error of our experimental value, but the predicted number for Cu^+ is higher than the value determined from ITC measurements. While this could reflect one or more discrepancies in the reported $\text{p}K_a$ values used for the proton inventory, computational results on the electrostatic properties of azurin suggest a number of small shifts in the $\text{p}K_a$'s of additional residues between the apo, reduced, and oxidized forms that are not included in the proton inventory.³⁶ Our experimentally determined values quantify the net proton displacement from all residues in the protein upon Cu^{2+} and Cu^+ binding.

a. Cu^{2+} Binding. In contrast to the biphasic Cu^{2+} binding reported earlier for titrations of apo–azurin into Cu^{2+} , the injection peaks for titrations of Cu^{2+} into apo–azurin indicate a single binding step under these conditions. The affinity of azurin for Cu^{2+} determined from our data is 2 orders of magnitude higher than reported previously,¹⁶ with binding

thermodynamics that are significantly different and unexpected. Although the coordination involves two His imidazoles that form strong bonds with Cu^{2+} and significantly covalent bonding with the Cys thiolate,³⁷ the net binding enthalpy is weakly endothermic ($\Delta H^{\circ'} = 2 \pm 1 \text{ kcal/mol}$).

Contributions to the Cu^{2+} binding enthalpy can be considered in a simple Hess's Law analysis (Scheme 1), which assumes that Cu^{2+} bonds to the protein residues, relative to the aqua ligands of $\text{Cu}^{2+}_{(\text{aq})}$, are the major contribution to the binding enthalpy.

Scheme 1. Hess's Law Analysis of the Enthalpy of Cu^{2+} Binding to Azurin

$\text{Cu}^{2+}_{(\text{aq})} + \text{Azurin} \rightleftharpoons \text{Cu}^{2+}\text{Azurin} + 1.5 (\pm 0.3) \text{ H}^+$	$\Delta H^{\circ'} = 2 \pm 1 \text{ kcal/mol}$
$\text{Cys112H} \rightleftharpoons \text{Cys112}^- + \text{H}^+$	$\Delta H_1 = +8.5 \text{ kcal/mol}$
$\text{His117H}^{+0.80} \rightleftharpoons \text{His117} + 0.80 \text{ H}^+$	$\Delta H_2 = 0.80 \times (+8.7 \text{ kcal/mol})$
$\text{His83H}^{+0.70} + 0.06 \text{ H}^+ \rightleftharpoons \text{His83H}^{+0.76}$	$\Delta H_3 = 0.06 \times (-8.7 \text{ kcal/mol})$
$\text{Cu}^{2+}_{(\text{aq})} + \text{His46} \rightleftharpoons \text{Cu}^{2+}\text{His46}$	$\Delta H_4 = -4.0 \text{ kcal/mol}$
$\text{Cu}^{2+}_{(\text{aq})} + \text{His117} \rightleftharpoons \text{Cu}^{2+}\text{His117}$	$\Delta H_5 = -4.0 \text{ kcal/mol}$
$\text{Cu}^{2+}_{(\text{aq})} + \text{Cys112}^- \rightleftharpoons \text{Cu}^{2+}\text{Cys112}^-$	$\Delta H_6 = ? \text{ kcal/mol}$
$\text{Cu}^{2+}_{(\text{aq})} + \text{Met121/C=O} \rightleftharpoons \text{Cu}^{2+}\text{Met121/C=O}$	$\Delta H_7 = ? \text{ kcal/mol}$

An estimate for the enthalpy of Cu^{2+} bonding to a His imidazole (-4 kcal/mol) is based on previous calorimetric measurements of Cu^{2+} binding to amino acids ($\sim -4.5 \text{ kcal/mol}$ from comparison of the CuL_2 formation enthalpies, where $\text{L} = \text{His, Gly, Ala}$),³⁸ a tetra-His peptide (-2.5 kcal/mol),³⁹ a series of His \rightarrow Ala variants of amyloid beta peptides (-2.5 to -5.0 kcal/mol),⁴⁰ and the three His residues in the active site of carbonic anhydrase (-5.8 kcal/mol , although this does not account for enthalpic contributions from accompanying Cu^{2+} –hydroxo bonding).⁴¹ The enthalpic penalty to deprotonate Cys112 and the 80% protonated His117 at pH 7.0 is included in the analysis, as is the small (0.5 kcal/mol) contribution due to partial protonation of His83 from a small shift in its pK_a upon Cu^{2+} binding. The long axial bonding⁸ to the thioether of Met121 (3.1 Å) and the backbone carbonyl of Gly45 (3.0 Å) is noted in the scheme but not included in the analysis because these bonding interactions have been estimated to be a fraction of that of a typical Cu^{2+} coordination bond.⁴² Since an estimate for the Cu^{2+} –thiolate bond enthalpy is not available, particularly for one as unique as the Cu^{2+} –Cys bond in azurin and other blue copper (type 1) sites, we use this analysis to estimate the enthalpy of this well-characterized bonding interaction.³⁷ This leads to an estimate of $\sim -5 \pm 2 \text{ kcal/mol}$ for the Cu^{2+} –Cys112 thiolate bond enthalpy, which is unremarkable for such a short (2.25 Å) and covalent bond. This value is not dissimilar from that of a typical Zn^{2+} –thiolate bond enthalpy,⁴³ as predicted by the Irving–Williams series.⁴⁴

The binding of Cu^{2+} to azurin is due to an extremely favorable net binding entropy ($-T\Delta S^{\circ'} = -23 \pm 1 \text{ kcal/mol}$ at 298 K) from desolvation of the Cu^{2+} ion and the active site and loss of ~ 1.5 protons from protein residues. This value reflects the lack of a conformational entropic penalty for binding to a protein site that is structurally very similar in its apo- and Cu^{2+} -bound forms (Figure 1). The earlier ITC study of Cu^{2+} binding to azurin estimated the entropy of binding with an analysis that included desolvation of the Cu^{2+} , change in protein conformation (assumed negligible), and the cratic entropy (2 particles \rightarrow 1 particle).¹⁶ This theoretical analysis

gave an estimated value of $\Delta S^{\circ'} = 29 \text{ cal/mol}\cdot\text{K}$, which is considerably smaller than the $\Delta S^{\circ'} = 78 \pm 3 \text{ cal/mol}\cdot\text{K}$ determined experimentally here. Additional contributions to the binding entropy that would increase the estimated value are loss of a water molecule from approximately half of the apo sites¹⁴ ($\sim 4.25 \text{ cal/mol}\cdot\text{K}$) and explicit consideration of the loss of 1.5 ± 0.3 protons and their contribution to the cratic entropy (2 particles $\rightarrow 2.5 \pm 0.3$ particles), which would now be positive. Measurements of $\Delta C_p^{\circ'}$ for Cu^{2+} binding to azurin would provide additional insight into solvation contributions to the binding entropy.

b. Cu^+ Binding. This is the first direct experimental quantification of the thermodynamics of Cu^+ binding to a protein. We find that azurin binds Cu^+ with a very favorable binding enthalpy ($\Delta H^{\circ'} = -17 \pm 1 \text{ kcal/mol}$) and a modestly favorable binding entropy ($-T\Delta S^{\circ'} = -7 \pm 1 \text{ kcal/mol}$ at 298 K). Relative to the entropically driven binding of Cu^{2+} , this is due to (a) coordination at a hydrophobic protein site that imposes a coordination geometry more commonly found with the d^{10} Cu^+ ion, (b) displacement of fewer net protons, which results in a smaller enthalpic penalty but a smaller entropic benefit, from an increase in the pK_a of His83 ($\Delta\text{p}K_a = 0.36 \pm 0.02$) and especially His35 ($\Delta\text{p}K_a = 0.8 \pm 0.2$) upon Cu^+ binding (Table S3), and (c) smaller desolvation of the monopositive Cu^+ than the dipositive Cu^{2+} , which reduces the enthalpic penalty (Cu^{2+} , $\Delta H_{\text{dehyd}} = 507 \text{ kcal/mol}$; Cu^+ , $\Delta H_{\text{dehyd}} = 140 \text{ kcal/mol}$) but also reduces the entropic benefit (Cu^{2+} , $\Delta S_{\text{dehyd}} = 81 \text{ cal/mol}\cdot\text{K}$; Cu^+ , $\Delta S_{\text{dehyd}} = 39 \text{ cal/mol}\cdot\text{K}$).⁴⁵

As with Cu^{2+} , a simple Hess's Law analysis (Scheme 2), which assumes that Cu^+ bonds to the protein residues, relative to the aqua ligands of $\text{Cu}^+_{(\text{aq})}$, are the major contribution to the binding enthalpy, provides additional insight.

Scheme 2. Hess's Law Analysis of the Enthalpy of Cu^+ Binding to Azurin

$\text{Cu}^+_{(\text{aq})} + \text{Azurin} \rightleftharpoons \text{Cu}^+\text{Azurin} + 0.6 (\pm 0.1) \text{ H}^+$	$\Delta H^{\circ'} = -17 \pm 1 \text{ kcal/mol}$
$\text{Cys112H} \rightleftharpoons \text{Cys112}^- + \text{H}^+$	$\Delta H_1 = +8.5 \text{ kcal/mol}$
$\text{His117H}^{+0.80} \rightleftharpoons \text{His117} + 0.80 \text{ H}^+$	$\Delta H_2 = 0.80 \times (+8.7 \text{ kcal/mol})$
$\text{His83H}^{+0.70} + 0.14 \text{ H}^+ \rightleftharpoons \text{His83H}^{+0.84}$	$\Delta H_3 = 0.14 \times (-8.7 \text{ kcal/mol})$
$\text{His35H}^{+0.24} + 0.45 \text{ H}^+ \rightleftharpoons \text{His35H}^{+0.69}$	$\Delta H_4 = 0.45 \times (-8.7 \text{ kcal/mol})$
$\text{Cu}^+_{(\text{aq})} + \text{Azurin site} \rightleftharpoons \text{Cu}^+\text{Azurin site}$	$\Delta H_5 = ? \text{ kcal/mol}$

Unfortunately, neither Cu^+ –His(imidazole) nor Cu^+ –Cys(thiolate) bond enthalpies have been reported. However, accounting for contributions from the protonation enthalpies of key residues and the known 1.2 displaced protons allows the overall bonding enthalpy of Cu^+ at the azurin site to be estimated at -27 kcal/mol . A similar estimate that uses the experimentally determined loss of only 0.6 ± 0.1 protons upon Cu^+ binding would include additional protonation enthalpies and reduce this value somewhat. However, either value is considerably more favorable than the -13 kcal/mol overall bonding enthalpy of Cu^{2+} at the azurin site from Scheme 1. Thus, this analysis quantifies the significantly more favorable overall bonding enthalpy of Cu^+ than Cu^{2+} at the blue copper site.⁴⁶

Reduction Thermodynamics from Calorimetric Measurements. Metalloproteins, such as those containing a blue copper site, have an intrinsic reduction potential that is set by the metal coordination to the protein (1st sphere) and the environment of the metal site (2nd sphere) to provide the

Table 5. Reduction Thermodynamic Values for Azurin at 25 °C and pH 7.0

ΔH_{E° (kcal/mol)	ΔG_{E° (kcal/mol)	E° (mV)	ΔS_{E° (cal/(mol K))	method	reference
-16.6 ± 0.4	-7.1 ± 0.1	308 ± 2	-31.7 ± 1.2	spectroelectro-chemistry	17
-16.4 ± 0.5	-7.1	307	-31.1 ± 2.0	CV	47
-15.4 ± 0.6	-6.7 ± 0.1	292 ± 2	-29.0 ± 0.2	spectroelectro-chemistry	50 ^a
-22.0 ± 1.4	-6.4 ± 0.4	279 ± 16	-52 ± 5	ITC	this work

^apH 8.0.

driving force ($\Delta G^{\circ'}_{E^\circ}$) for electron transfer. The reduction free energy originates from the enthalpic ($\Delta H^{\circ'}_{E^\circ}$) and entropic ($\Delta S^{\circ'}_{E^\circ}$) contributions (eq 6)

$$\Delta G^{\circ'}_{E^\circ} = -nFE^\circ = \Delta H^{\circ'}_{E^\circ} - T\Delta S^{\circ'}_{E^\circ} \quad (6)$$

but the connection between these thermodynamic components and the properties of the protein is not well understood. The initial and final states of electron transfer to the protein include the metal cofactor in its oxidized and reduced states, respectively, which have different coordination thermodynamics at the protein site due to a different electronic configuration and charge. Further, the electrostatic changes that accompany electron transfer typically result in a coupled proton transfer, which contributes to the overall thermodynamics of reduction.

The reduction thermodynamics can be determined from the temperature dependence of the reduction potential and analysis with the Gibbs–Helmholtz relationship. Values for *Pseudomonas aeruginosa* azurin and other metalloproteins were initially reported by Gray, Anson, and co-workers, who used spectroelectrochemical measurements with an optically transparent thin-layer electrochemical (OTTLE) cell and outlined the assumptions that connect the experimental $\Delta S^{\circ'}_{rc}$ value to a standard state $\Delta S'$ value.¹⁷ Subsequently, Sola and co-workers confirmed and extended these results with cyclic voltammetry (CV) electrochemical measurements on a number of blue copper proteins.⁴⁷ These methods require the assumption that $\Delta S^{\circ'}_{rc}$ and $\Delta H^{\circ'}_{rc}$ are constant over the experimental temperature range, but this can be a tenuous assumption for proteins in aqueous solution, where binding is typically associated with a significant change in the heat capacity.^{48,49} Direct calorimetric measurements at a single temperature eliminate the need for these assumptions.

In this study, we have used ITC to quantify the thermodynamics of both Cu^{2+} and Cu^+ binding to azurin, which were then used in thermodynamic cycles to determine the reduction thermodynamics of the metalloprotein. These results are comparable to those obtained from temperature-dependent electrochemical measurements (Table 5), which show that reduction is enthalpically favored with an unfavorable change in entropy.^{17,47}

The former is generally attributed to electronic factors associated with differences in bond enthalpies between the two metal ions, while the latter is generally dominated by differences in solvation between the oxidized and reduced proteins.

The calorimetric method to determine metalloprotein reduction thermodynamics, which was evaluated here and is designated redox coordination thermodynamics (RCT), has certain advantages and unique capabilities. First, thermodynamic values are obtained at a single temperature and do not require assumptions about their temperature independence. This is one possible source of differences between values obtained with temperature-dependent electrochemical measurements and the calorimetric values (Table 5). Differences

between the ionic strength of the electrochemical and calorimetry solutions may also contribute to these discrepancies. Second, direct measurement of the binding thermodynamics for each oxidation state of the metal provides quantitative insight about contributions from the oxidized and reduced forms to the reduction thermodynamics, as discussed below for azurin. Third, the metal-binding data can be used to quantify the proton transfer that is associated with reduction of the metalloprotein, also discussed below for azurin.

The binding thermodynamics of the oxidized and reduced metal ion indicate key properties of the initial and final states of metalloprotein reduction, which determines the change in enthalpy and entropy for electron transfer. In the case of azurin, Cu^{2+} binding to the protein is entirely due to favorable entropic contributions with a small net enthalpic penalty, while Cu^+ has a very favorable net binding enthalpy and is also favored entropically. These metal-binding thermodynamics can be correlated to the reduction of azurin, which has a favorable change in enthalpy ($\Delta H^{\circ'}_{E^\circ} = -22 \pm 1$ kcal/mol), due to the large difference in binding enthalpy that favors Cu^+ over Cu^{2+} , which overcomes a disfavorable change in entropy ($-T\Delta S^{\circ'}_{E^\circ} = 15.5 \pm 1.5$ kcal/mol at 298 K) when the entropically favored Cu^{2+} is reduced to Cu^+ .

To determine the condition-independent change in enthalpy from calorimetry measurements of a metal ion binding to a protein, it is essential to quantify and account for any loss (gain) of proton(s) to (from) the buffer that is coupled to metal binding. The difference between these values for the two metal oxidation states quantifies the difference in protonation of the metalloprotein between its oxidized and reduced forms and thus the proton transfer that accompanies the electron transfer. Analysis of the ITC data reveals that 0.9 ± 0.3 protons bind to azurin upon its reduction at pH 7.0. Proton transfer that accompanies reduction can also be determined from a proton inventory based on the experimentally determined pK_a values of key residues in the oxidized and reduced protein, when these values are known, as they are for azurin.^{20,35} This analysis predicts that 0.5 ± 0.1 protons bind to azurin upon its reduction. The value determined by ITC, however, includes protonation and deprotonation contributions from all protein residues and is consistent with the pH dependence of the azurin reduction potential^{35,50,51} and computational results that ~ 0.85 protons bind upon reduction at pH 7.0.³⁶

Protein Tuning of the Reduction Potential. The RCT method validated here to quantify metalloprotein reduction thermodynamics provides new insight about contributions from the initial and final states of electron transfer and has the potential to provide important insight about protein tuning of the reduction potential in metalloenzymes, such as tyramine β -monooxygenase⁵² and polysaccharide monooxygenase.⁵³ As a first step in the application of this method, preliminary ITC data for Cu^{2+} and Cu^+ binding to the low-potential F114P variant of azurin⁵⁴ have been obtained. Its reduction

thermodynamics reveal that the lower potential is due to a significant drop in the favorable reduction enthalpy and a corresponding, but smaller, drop in the unfavorable reduction entropy (Table 4). This reflects a partial enthalpy–entropy compensation (EEC), as found with electrochemical measurements on other azurin variants.^{51,55}

The impact of this mutation on the Cu²⁺ and Cu⁺ binding thermodynamics (Table 3) reveals additional new insight. Loss of one of the two hydrogen bonds to Cys112 in the F114P variant leads to a more nucleophilic thiolate ligand that bonds with greater covalency to the Cu²⁺⁵⁶ and a binding that is found here to be 11 kcal/mol more exothermic than binding to wild-type azurin. However, this is entirely canceled by a loss of binding entropy, resulting in no change in the protein affinity for Cu²⁺. The loss of entropy, relative to Cu²⁺ binding to wild-type azurin, may be due to the stronger Cu²⁺–thiolate bond in the variant and a general rigidification of the active site, since the remaining hydrogen bond to Cys112 becomes shorter and stronger, as does the axial Met121 bond to Cu²⁺.⁵⁴ Alternatively, the unfavorable entropy for Cu²⁺ binding to F114P, relative to wild-type azurin, may originate from loss of the phenyl ring of Phe114. Four additional water molecules occupy the resulting cavity, including one that is hydrogen-bonded to the backbone carbonyl of Gly45 and only 5.6 Å from the Cu²⁺.⁵⁴ Loss of the hydrogen bond to Cys112 increases the covalency of the sulfur–copper bonding, as quantified by X-ray absorption measurements, and introduces an electrostatic contribution that together are predicted to lower the reduction potential by ~250 mV.⁵⁶ Since the reduction potential decreases only ~100 mV, which corresponds to the contribution from the increased covalency, it has been suggested that the dipoles of these waters oppose and cancel the electrostatic contribution.⁵⁶ Therefore, the loss of translational and rotational entropy of these nearby waters upon Cu²⁺ binding to F114P azurin may provide an entropic penalty that cancels the more favorable enthalpy of Cu²⁺ binding to this variant.

Loss of the hydrogen bond to Cys112 in F114P does have a net effect on the protein affinity for Cu⁺, resulting in a weaker binding that is less exothermic by 4 kcal/mol and only partially compensated by a more favorable binding entropy ($-T\Delta\Delta S^\circ = -1.5$ kcal/mol at 298 K). Thus, the drop in the reduction potential of F114P, relative to wild-type azurin, is due to a decrease in the reduction enthalpy from both a less exothermic Cu⁺ binding and a more exothermic Cu²⁺ binding. However, a significant decrease in the Cu²⁺ binding entropy partially cancels the enthalpic factors that lower the reduction potential of this variant. The net result is that F114P binds Cu⁺ less tightly but Cu²⁺ with the same overall affinity as wild-type azurin. New molecular insight, such as this, is expected from ITC measurements and analysis with the RCT method on other azurin variants with lower and higher potentials⁵⁷ and on Cu-containing metalloenzymes currently in progress.

ASSOCIATED CONTENT

Supporting Information

The Supporting Information is available free of charge on the ACS Publications website at DOI: [10.1021/jacs.9b06836](https://doi.org/10.1021/jacs.9b06836).

Procedures for protein expression and purification; representative ITC data and analysis to determine the thermodynamics of Cu²⁺–buffer interactions (Appendix A) and the formation thermodynamics of Cu⁺–

Me₆Trien (Appendix B); enthalpy plots to determine proton displacement upon Cu²⁺ and Cu⁺ binding to azurin; representative ITC data, fit parameters, and thermodynamics of Cu²⁺ and Cu⁺ binding to F114P azurin (PDF)

AUTHOR INFORMATION

Corresponding Author

*dean.wilcox@dartmouth.edu

ORCID

Dean E. Wilcox: [0000-0003-2061-4838](https://orcid.org/0000-0003-2061-4838)

Present Address

[†]Avitide, Lebanon, NH 03766

Notes

The authors declare no competing financial interest.

ACKNOWLEDGMENTS

We are grateful to Yi Lu for providing the expression systems for native azurin and the F114P variant and for valuable discussions. We thank Ekaterina Pletneva for valuable discussions and helpful advice about azurin expression and purification. We thank the NSF (CHE-1609553 and CHE-1308598; “Thermodynamics of Metal–Protein Interactions”) for support of this research.

REFERENCES

- (1) Banci, L.; Bertini, I.; Luchinat, C.; Turano, P. Electron-Transfer Proteins. In *Biological Inorganic Chemistry*; Bertini, I., Gray, H. B., Stiefel, E. I., Valentine, J. S., Eds.; University Science: Sausalito, 2007; pp 229–261.
- (2) Stubbe, J.; Nocera, D. G.; Yee, C. S.; Chang, M. C. Y. Radical Initiation in the Class 1 Ribonucleotide Reductase: Long-Range Proton-Coupled Electron Transfer? *Chem. Rev.* **2003**, *103*, 2167–2201.
- (3) Huynh, M. H. V.; Meyer, T. J. Proton-Coupled Electron Transfer. *Chem. Rev.* **2007**, *107*, 5004–5064.
- (4) Warren, J. J.; Tronic, T. A.; Mayer, J. M. Thermochemistry of Proton-Coupled Electron Transfer Reagents and Its Implications. *Chem. Rev.* **2010**, *110*, 6961–7001.
- (5) Dempsey, J. L.; Winkler, J. R.; Gray, H. B. Proton-Coupled Electron Flow in Protein Redox Machines. *Chem. Rev.* **2010**, *110*, 7024–7039.
- (6) Hammes-Schiffer, S. Proton-Coupled Electron Transfer: Moving Together and Charging Forward. *J. Am. Chem. Soc.* **2015**, *137*, 8860–8871.
- (7) Freeman, H. C.; Guss, J. M. Plastocyanin. In *Handbook of Metalloproteins*; Messerschmidt, A., Huber, R., Poulos, T., Wieghardt, K., Eds.; Wiley: Chichester, 2001; Vol. 2, pp 1153–1169.
- (8) Kolczak, U.; Dennison, C.; Messerschmidt, A.; Canters, G. W. Azurin and Azurin Mutants. In *Handbook of Metalloproteins*; Messerschmidt, A., Huber, R., Poulos, T., Wieghardt, K., Eds.; Wiley: Chichester, 2001; Vol. 2, pp 1170–1194.
- (9) Davies, G. J.; Ducros, V. Laccase. In *Handbook of Metalloproteins*; Messerschmidt, A., Huber, R., Poulos, T., Wieghardt, K., Eds.; Wiley: Chichester, 2001; Vol. 2, pp 1359–1368.
- (10) Messerschmidt, A. Ascorbate Oxidase. In *Handbook of Metalloproteins*; Messerschmidt, A., Huber, R., Poulos, T., Wieghardt, K., Eds.; Wiley: Chichester, 2001; Vol. 2, pp 1345–1358.
- (11) Guss, J. M.; Harrowell, P. M.; Murata, M.; Norris, V. A.; Freeman, H. C. Crystal Structure Analyses of Reduced (CuI) Poplar Plastocyanin at Six pH Values. *J. Mol. Biol.* **1986**, *192*, 361–387.
- (12) Shepard, W. B.; Anderson, B. F.; Lewandoski, D. A.; Norris, G. E.; Baker, E. N. Copper Coordination Geometry in Azurin Undergoes Minimal Change On Reduction of Copper(II) to Copper(I). *J. Am. Chem. Soc.* **1990**, *112*, 7817–7819.

(13) Garrett, T. P. J.; Clingleffer, D. J.; Guss, J. M.; Rogers, S. J.; Freeman, H. C. The Crystal Structure of Poplar Apoplastocyanin at 1.8 Å Resolution. The Geometry of the Copper-Binding Site is Created by the Polypeptide. *J. Biol. Chem.* **1984**, *259*, 2822–2825.

(14) Nar, H.; Messerschmidt, A.; Huber, R.; van de Kamp, M.; Canters, G. W. Crystal Structure of *Pseudomonas aeruginosa* Apo-Azurin at 1.85 Å Resolution. *FEBS Lett.* **1992**, *306*, 119–124.

(15) Shepard, W. B.; Kingston, R. L.; Anderson, B. F.; Baker, E. N. Structure of Apo-Azurin from *Alcaligenes denitrificans* at 1.8 Angstrom Resolution. *Acta Crystallogr., Sect. D: Biol. Crystallogr.* **1993**, *49*, 331–343.

(16) Blasie, C. A.; Berg, J. M. Kinetics and Thermodynamics of Copper(II) Binding to Apoazurin. *J. Am. Chem. Soc.* **2003**, *125*, 6866–6867.

(17) Taniguchi, V.; Sailasuta-Scott, N.; Anson, F. C.; Gray, H. B. Thermodynamics of Metalloprotein Electron Transfer Reactions. *Pure Appl. Chem.* **1980**, *52*, 2275–2281.

(18) Battistuzzi, G.; Borsari, M.; Di Rocco, G.; Ranieri, A.; Sola, M. Enthalpy/Entropy Compensation Phenomena in the Reduction Thermodynamics of Electron Transport Metalloproteins. *JBIC, J. Biol. Inorg. Chem.* **2004**, *9*, 23–26 and references therein.

(19) Karlsson, B. G.; Pascher, T.; Nordling, M.; Arvidsson, R. H.; Lundberg, L. G. Expression of the Blue Copper Protein Azurin from *Pseudomonas aeruginosa* in *Escherichia coli*. *FEBS Lett.* **1989**, *246*, 211–217.

(20) van de Kamp, M.; Hali, F. C.; Rosato, N.; Agro, A. F.; Canters, G. W. Purification and Characterization of a Non-Reconstitutable Azurin, Obtained by Heterologous Expression of the *Pseudomonas aeruginosa* Azu Gene in *Escherichia coli*. *Biochim. Biophys. Acta, Bioenerg.* **1990**, *1019*, 283–292.

(21) Sutherland, I. W.; Wilkinson, J. F. Azurin: A Copper Protein Found in Bordetella. *J. Gen. Microbiol.* **1963**, *30*, 105–112.

(22) Wittung-Stafshede, P.; Hill, M. G.; Gomez, E.; Di Bilio, A. J.; Karlsson, B. G.; Leckner, J.; Winkler, J. R.; Gray, H. B.; Malstrom, B. G. Reduction Potentials of Blue and Purple Copper Proteins in Their Unfolded States: A Closer Look at Rack-Induced Coordination. *JBIC, J. Biol. Inorg. Chem.* **1998**, *3*, 367–370.

(23) Johnson, D. K.; Stevenson, M. J.; Almadidy, Z. A.; Jenkins, S. E.; Wilcox, D. E.; Grossoehme, N. E. Stabilization of Cu(I) for Binding and Calorimetric Measurements in Aqueous Solution. *Dalton Trans* **2015**, *44*, 16494–16505.

(24) Xiao, Z.; Donnelly, P. S.; Zimmermann, M.; Wedd, A. G. Transfer of Copper between Bis(thiosemicarbazone) Ligands and Intracellular Copper-Binding Proteins. Insights into Mechanisms of Copper Uptake and Hypoxia Selectivity. *Inorg. Chem.* **2008**, *47*, 4338–4347.

(25) Grossoehme, N. E.; Spuches, A. M.; Wilcox, D. E. Application of Isothermal Titration Calorimetry in Bioinorganic Chemistry. *JBIC, J. Biol. Inorg. Chem.* **2010**, *15*, 1183–1191.

(26) Goldberg, R. N.; Kishore, N.; Lennen, R. M. Thermodynamic Quantities for the Ionization Reactions of Buffers. *J. Phys. Chem. Ref. Data* **2002**, *31*, 231–370.

(27) Golub, G.; Cohen, H.; Paoletti, P.; Bencini, A.; Messori, L.; Bertini, I.; Meyerstein, D. Use of Hydrophobic Ligands for the Stabilization of Low-Valent Transition Metal Complexes. 1. The Effect of N-Methylation of Linear Tetraazaalkane Ligands on the Properties of Their Copper Complexes. *J. Am. Chem. Soc.* **1995**, *117*, 8353–8361.

(28) Latimer, W. M. *Oxidation Potentials*, 2nd ed.; Prentice-Hall: Englewood Cliffs, 1952.

(29) Marshall, N. M.; Garner, D. K.; Wilson, T. D.; Gao, Y.-G.; Robinson, H.; Nilges, M. J.; Lu, Y. Rationally Tuning the Reduction Potential of a Single Cupredoxin Beyond the Natural Range. *Nature* **2009**, *462*, 113–117.

(30) North, M. L.; Zawisza, I.; Bal, W.; Wilcox, D. E., unpublished results.

(31) Pappalardo, M.; Sciacca, M. F. M.; Milardi, D.; Grasso, D. M.; La Rosa, C.; Catania, S.; Doria, V. A. Thermodynamics of Azurin Folding. The Role of Copper Ion. *J. Therm. Anal. Calorim.* **2008**, *93*, 575–581.

(32) Pappalardo, M.; Milardi, D.; Grasso, D. M.; La Rosa, C. Free Energy Perturbation and Molecular Dynamics Calculations of Copper Binding to Azurin. *J. Comput. Chem.* **2003**, *24*, 779–785.

(33) Wittung-Stafshede, P. Role of Cofactors in Folding of the Blue-Copper Protein Azurin. *Inorg. Chem.* **2004**, *43*, 7926–7933.

(34) Badarau, A.; Dennison, C. Thermodynamics of Copper and Zinc Distribution in the Cyanobacterium *Synechocystis* PCC 6903. *Proc. Natl. Acad. Sci. U. S. A.* **2011**, *108*, 13007–13012.

(35) van de Kamp, M.; Canters, G. W.; Andrew, C. R.; Sanders-Loehr, J.; Bender, C. J.; Peisach, J. Effect of Lysine Ionization on the Structure and Electrochemical Behaviour of the Met44→Lys Mutant of the Blue-Copper Protein Azurin. *Eur. J. Biochem.* **1993**, *218*, 229–238.

(36) Ullmann, R. T.; Ullmann, G. M. Coupling of Protonation, Reduction and Conformational Change in Azurin from *Pseudomonas aeruginosa* Investigated with Free Energy Measures of Cooperativity. *J. Phys. Chem. B* **2011**, *115*, 10346–10359.

(37) Solomon, E. I.; Hadt, R. G. Recent Advances in Understanding Blue Copper Proteins. *Coord. Chem. Rev.* **2011**, *255*, 774–789.

(38) Stack, W. F.; Skinner, H. A. Microcalorimetry Studies. Heats of Complexing of Transition Metal Ions with Amino-Acids. *Trans. Faraday Soc.* **1967**, *63*, 1136–1145.

(39) Grossoehme, N. G.; Akilesh, S.; Guerinot, M. L.; Wilcox, D. E. Metal-Binding Thermodynamics of the Histidine-Rich Sequence from the Metal-Transport Protein IRT1 of *Arabidopsis thaliana*. *Inorg. Chem.* **2006**, *45*, 8500–8508.

(40) Hong, L.; Carducci, T. M.; Bush, W. D.; Dudzik, C. G.; Millhauser, G. L.; Simon, J. D. Quantification of the Binding Properties of Cu²⁺ to the Amyloid Beta Peptide: Coordination Spheres for Human and Rat Peptides and Implication on Cu²⁺-Induced Aggregation. *J. Phys. Chem. B* **2010**, *114*, 11261–11271.

(41) Nettles, W. L.; Song, H.; Farquhar, E. R.; Fitzkee, N. C.; Emerson, J. P. Characterization of Copper(II) Binding Sites in Human Carbonic Anhydrase II. *Inorg. Chem.* **2015**, *54*, 5671–5680.

(42) Lowery, M. D.; Solomon, E. I. Axial Ligand Bonding in Blue Copper Proteins. *Inorg. Chim. Acta* **1992**, *198–200*, 233–243.

(43) Rich, A. M.; Bombarda, E.; Schenk, A. D.; Lee, P. E.; Cox, E. H.; Spuches, A. M.; Hudson, L. D.; Keiffer, B.; Wilcox, D. E. Thermodynamics of Zn²⁺ Binding to Cys₂His₂ and Cys₂HisCys Zinc Fingers and a Cys₄ Transcription Factor Site. *J. Am. Chem. Soc.* **2012**, *134*, 10405–10418.

(44) Irving, H.; Williams, R. J. P. Order of Stability of Metal Complexes. *Nature* **1948**, *162*, 746–747.

(45) Marcus, Y. A Simple Empirical Model Describing the Thermodynamics of Hydration of Ions of Widely Varying Charges, Sizes and Shapes. *Biophys. Chem.* **1994**, *51*, 111–127.

(46) Guckert, J. A.; Lowery, M. D.; Solomon, E. I. Electronic Structure of the Reduced Blue Copper Active Site: Contributions to Reduction Potentials and Geometry. *J. Am. Chem. Soc.* **1995**, *117*, 2817–2844.

(47) Battistuzzi, G.; Borsari, M.; Loschi, L.; Righi, F.; Sola, M. Redox Thermodynamics of Blue Copper Proteins. *J. Am. Chem. Soc.* **1999**, *121*, 501–506.

(48) Sturtevant, J. M. Heat Capacity and Entropy Changes in Processes Involving Proteins. *Proc. Natl. Acad. Sci. U. S. A.* **1977**, *74*, 2236–2240.

(49) Prabhu, N. V.; Sharp, K. A. Heat Capacity in Proteins. *Annu. Rev. Phys. Chem.* **2005**, *56*, 521–548.

(50) St Clair, C. S.; Ellis, W. R., Jr.; Gray, H. B. Spectroelectrochemistry of Blue Copper Proteins: pH and Temperature Dependences of the Reduction Potentials of Five Azurins. *Inorg. Chim. Acta* **1992**, *191*, 149–155.

(51) Battistuzzi, G.; Borsari, M.; Canters, G. W.; de Waal, E.; Loschi, L.; Warmerdam, G.; Sola, M. Enthalpic and Entropic Contributions to the Mutational Changes in the Reduction Potential of Azurin. *Biochemistry* **2001**, *40*, 6707–6712.

(52) Zhu, H.; Sommerhalter, M.; Nguy, A.; Klinman, J. P. Solvent and Temperature Probes of the Long-Range Electron-Transfer Step in Tyramine R-Monooxygenase: Demonstration of a Long-Range Proton-Coupled Electron-Transfer Mechanism. *J. Am. Chem. Soc.* **2015**, *137*, 5720–5729.

(53) Kjaergaard, C. H.; Qayyum, M. F.; Wong, S. D.; Xu, F.; Hemsworth, G. R.; Walton, D. J.; Young, N. A.; Davies, G. J.; Walton, P. H.; Johansen, K. S.; Hodgson, K. O.; Hedman, B.; Solomon, E. I. Spectroscopic and Computational Insight into the Activation of O₂ by the Mononuclear Cu Center in Polysaccharide Monooxygenases. *Proc. Natl. Acad. Sci. U. S. A.* **2014**, *111*, 8797–8802.

(54) Yanagisawa, S.; Banfield, M. J.; Dennison, C. The Role of Hydrogen Bonding at the Active Site of a Cupredoxin: The Phe114Pro Azurin Variant. *Biochemistry* **2006**, *45*, 8812–8822.

(55) Battistuzzi, G.; Bellei, M.; Borsari, M.; Canters, G. W.; de Waal, E.; Jeuken, L. J. C.; Ranieri, A.; Sola, M. Control of Metalloprotein Reductions Potential: CompensationPhenomena in the Reduction Thermodynamics of Blue Copper Proteins. *Biochemistry* **2003**, *42*, 9214–9220.

(56) Hadt, R. G.; Sun, N.; Marshall, N. M.; Hodgson, K. O.; Hedman, B.; Lu, Y.; Solomon, E. I. Spectroscopic and DFT Studies of Second-Sphere Variants of the Type 1 Copper Site in Azurin: Covalent and Nonlocal Electrostatic Contributions to Reduction Potentials. *J. Am. Chem. Soc.* **2012**, *134*, 16701–16716.

(57) Hosseinzadeh, P.; Marshall, N. M.; Chacon, K. N.; Yu, Y.; Nilges, M. J.; New, S. Y.; Tashkov, S. A.; Blackburn, N. J.; Lu, Y. Design of a Single Protein That Spans the Entire 2-V Range of Physiological Redox Potentials. *Proc. Natl. Acad. Sci. U. S. A.* **2016**, *113*, 262–267.